Role of Oxysterol Structure on the Microdomain-Induced Microsolubilization of Phospholipid Membranes by Apolipoprotein A-I†

John B. Massey* and Henry J. Pownall

Section of Atherosclerosis and Lipoprotein Research, Department of Medicine, Baylor College of Medicine, One Baylor Plaza, Houston, Texas 77030

Received June 16, 2005; Revised Manuscript Received August 28, 2005

ABSTRACT: Oxygenated derivatives of cholesterol, oxysterols, have different physicochemical properties and three-dimensional shapes. The kinetics of microsolubilization of dimyristoylphosphatidylcholine (DMPC) multilamellar vesicles by apolipoprotein A-I (apoA-I) to form discoidal high-density lipoproteins (rHDL) was dramatically affected by oxysterol chemical structure. Under the experimental conditions of varying oxysterol chemical structure, sterol concentration, and the lipid phase state of DMPC, the kinetics varied over 3 orders of magnitude. Some oxysterols behaved similarly to cholesterol and increased the rate of microsolubilization; however, they were not as effective as cholesterol. Other oxysterols greatly inhibited this process. In general, there was no correlation of the rates with membrane fluidity as measured by fluorescence polarization. The rate of DMPC microsolubilization by apoA-I is highly dependent upon the presence of lattice defects in the membrane surface that occur due to imperfect packing of coexisting lipid phases. The differential ability of various oxysterols to induce the formation of an ordered lipid phase is the probable basis for their effects on the rates of DMPC microsolubilization. There was no effect of oxysterol chemical structure on the structure of the equilibrium rHDL products; however, there was a dramatic effect of sterol concentration on rHDL particle size. Different oxysterols regulate the kinetics of apoA-I membrane association by altering structural microheterogeneity at the membrane surface. However, once the kinetic barrier is overcome, the particle sizes of rHDL products formed are determined solely by the amount of sterol presence.

Oxysterols are intermediates or end products of cholesterol synthetic and catabolic pathways (*1*, *2*) and constitute one of the major toxic lipid classes in atherosclerotic plaques (*3*, *4*). Oxysterols are derivatives of cholesterol that contain a second oxygen atom as a carbonyl, hydroxyl, or epoxide group (*1*, *2*). Oxidative modifications of cholesterol generate sterols with different physicochemical properties (e.g., hydrophobicity) and three-dimensional shapes. Cholesterol has many effects on phospholipid bilayers. Cholesterol increases bilayer thickness, decreases membrane permeability, modulates acyl chain motion, decreases interfacial hydration, and forms L_o[1] microdomains or lipid rafts. The structural basis for the formation of L_o microdomains is the tight packing between cholesterol and lipids with saturated acyl chains, which maximizes favorable van der Waals interactions. The tighter the packing of a sterol, the more strongly it promotes microdomain formation. The effectiveness of a given sterol to form ordered lipid microdomains is dependent upon the location and chemical nature of substitutions on the sterol nucleus, which determine bulkiness, polarity, and membrane orientation, the number and location of double bonds which determine planarity, and the bulkiness and length of the hydrophobic side chain (*5*−*10*). The many different physiological oxysterols vary from cholesterol in at least one of these structural features. 7-Ketocholesterol and 25-hydroxycholesterol are lipid-domain-promoting sterols (*5*, *7*, *9*); however, other biologically active oxysterols have not been systematically studied. Oxysterols are less efficient at condensing or ordering fluid bilayers than cholesterol, suggesting that they should be less effective raft-forming lipids (*11*−*16*). In model membranes, sterol concentration and sterol structure determine the number and size of membrane domains (*17*) and whether they induce positive or negative membrane curvature (*18*). Microdomain formation also induces membrane surface heterogeneity, which is known to regulate the association of apolipoproteins (*19*−*24*), phospholipases (*25*, *26*), and other membrane-associating proteins with lipid surfaces (*27*). The formation, biophysical properties, and surface heterogeneity of different membrane microdomains are regulated by sterol chemical structure, sterol composition, and sterol concentration (*5*−*10*, *17*, *18*).

† Supported by grants from the National Institutes of Health (HL-30914 and HL-56865 to H.J.P.).

* To whom correspondence should be addressed. Phone: (713) 798-4141. Fax: (713) 798-4121. E-mail: jbm@bcm.tmc.edu.

[1] Abbreviations: apoA-I, apolipoprotein A-I, the major protein component of human high-density lipoproteins; DMPC, dimyristoyl-*sn*-glycero-3-phosphocholine; DPH, 1,6-diphenyl-1,3,5-hexatriene; DPPC, dipalmitoyl-*sn*-glycero-3-phosphocholine; 5α-Epo, 5α,6α-epoxycholesterol; 5β-Epo, 5β,6β-epoxycholesterol; 7β-HO, 7β-hydroxycholesterol; 20α-HO, 20α-hydroxycholesterol; 22R-HO, 22(*R*)-hydroxycholesterol; 24α-HO, 24α-hydroxycholesterol; 25-HO, 25-hydroxycholesterol; 27-HO, 27-hydroxycholesterol; HDL, high-density lipoproteins; L_d, liquid-disordered phase; L_o, liquid-ordered phase; LDL, low-density lipoprotein; MLV, multilamellar vesicles; PAGE, polyacrylamide gel electrophoresis; POPC, 1-palmitoyl-2-oleoyl-*sn*-glycero-3-phosphocholine; rHDL, reassembled HDL; T_M, midpoint temperature of the gel to liquid-disordered phase transition.

10.1021/bi051169y CCC: $30.25 © 2005 American Chemical Society
Published on Web 10/05/2005

High-density lipoproteins are protective against the development of atherosclerosis (*28*−*31*). One mechanism for the protective effects of HDL is reverse cholesterol transport. HDL transports excess cellular cholesterol from extrahepatic tissues, e.g., macrophage foam cells in atherosclerotic lesions, to the liver where it can be recycled or catabolized to bile acids, which are excreted. The initial step in HDL formation is the lipidation of apoA-I by the ABCA1 lipid transporter. This step is important in the hepatic formation of nascent HDL and also in the removal of excess cholesterol from macrophage foam cells. The detailed mechanism by which the ABCA1 transporter works is not known. However, one part of the mechanism appears to involve a microsolubilization step whereby lipid-poor apoA-I simultaneously removes phospholipid and cholesterol from cell surface lipid domains (*28*, *29*, *32*−*34*). We have reported a method that helps to identify factors, protein structure (*21*) and membrane biophysical properties (*19*, *20*, *22*, *23*), that regulate apolipoprotein−membrane association. This method is based on apoA-I-induced microsolubilization of DMPC MLV, which yields small discoidal rHDL that are similar to nascent HDL formed by the hepatic ABCA1 transporter pathway. However, for apoA-I to form rHDL with phospholipids that possess longer or more unsaturated acyl chains requires a detergent solubilization method to overcome the kinetic barrier that prevents lipid/protein complex formation. ApoA-I spontaneously forms rHDL with DMPC, and the use of this well-characterized lipid allows a mechanistic comparison of the kinetics of rHDL formation with the well-characterized phase properties of DMPC/cholesterol bilayers. 7-Ketocholesterol is an oxysterol that inhibits apoA-I-mediated cholesterol efflux from macrophages (*35*, *36*). The proposed mechanism is the disruption of apoA-I binding to plasma membrane lipid rafts. In this report, we describe the sterol-specific regulation of the kinetics of microsolubilization of DMPC MLV by apoA-I, finding that oxysterol structure determines the rate of microsolubilization in which certain oxysterols, e.g., 27-HO, are inhibitory. However, the resultant discoidal rHDL is mainly a function of sterol concentration, independent of the oxysterol structure, and similar in size to rHDL formed from apoA-I/cholesterol/DPPC mixtures using a cholate removal method (*37*) and to apoA-I-containing particles formed by ABCA1 (*33*, *38*).

EXPERIMENTAL PROCEDURES

Materials. 5α-Epoxycholesterol (cholestane-5α,6α-epoxy-3*β*-ol), 5*β*-epoxycholesterol (cholestane-5*β*,6*β*-epoxy-3*β*-ol), 7*β*-hydroxycholesterol (5-cholestene-3*β*,7*β*-diol), 20α-hydroxycholesterol (5-cholestene-3*β*,20α-diol), 22(*R*)-hydroxycholesterol [5-cholestene-3*β*,22(*R*)-diol], 24α-hydroxycholesterol [5-cholestene-3*β*,24(*S*)-diol], 25-hydroxycholesterol (5-cholestene-3*β*,25-diol), and 27-hydroxycholesterol [5,25-(*R*)-cholestene-3*β*,26-diol] were from Steraloids, Inc. (Newport, RI). DMPC was from Avanti Polar Lipids, Inc. (Alabaster, AL). DPH was from Molecular Probes, Inc. (Eugene, OR). High-purity cholesterol was from Calbiochem-Novabiochem (La Jolla, CA). ApoA-I was isolated from human plasma as previously described (*23*).

Liposome Preparation. The model membranes consisted of DMPC with either cholesterol or one of the different oxysterols. To prepare MLV with specific lipid compositions, the required amounts of phospholipid and sterol were originally mixed in chloroform/methanol (2/1 v/v). For the fluorescence experiments, the fluorescent probe was added at this stage at a ratio of 1/250 mol/mol probe/phospholipid. The organic solvent was evaporated under a stream of nitrogen, and the samples were dried overnight under vacuum in a lyophilizer. The dried lipids were dispersed in TBS buffer (100 mM NaCl, 10 mM Tris, 1 mM EDTA, 1 mM NaN_3, pH 7.4) by vortexing. To ensure complete hydration, the lipids were subjected to at least three freeze−thaw cycles which consisted of warming the samples to 37 °C, which was above the liquid-crystalline phase transition of DMPC, and freezing the samples at −20 °C.

Fluorescence Measurements. Fluorescence measurements were performed on a Jobin Yvon Spex Fluorolog-3 FL3-22 spectrofluorometer (Edison, NJ), which was equipped with Glan-Thompson polarizing prisms and a sample heater/cooler Peltier thermocouple drive. The fluorescence polarization of DPH was used to measure the effect of sterol structure on the acyl chain motion and phase properties of phospholipid bilayers (*39*); excitation and emission wavelengths were 350 and 425 nm, respectively. The fluorescence polarization (P) was calculated as $P = (I_{vv} - GI_{vh})/(I_{vv} + GI_{vh})$, where I_{vv} and I_{vh} represent the intensity of vertically and horizontally polarized fluorescent light, respectively, when the excitation light is vertically polarized. The correction factor $G = I_{hv}/I_{hh}$ was used to correct for the effect of the monochromator on the measured polarized light. I_{hv} and I_{hh} represent the intensity of vertically polarized and horizontally polarized light, respectively, when the excitation light is horizontally polarized. The fluorescence polarization, which includes a correction for the grating factor, was measured and calculated using an automated feature and vendor software. For thermal melting studies, the temperature was increased in 1 °C increments using the Peltier temperature controller, and the sample was equilibrated for 1 min, after which the polarization was recorded. The temperature profiles were fitted by a sigmoidal regression analysis (Sigma Plot 8.0) to obtain a value for the midpoint temperature (T_M) where a 50% change in the fluorescence values occurs. The equation used was $p(T) = p_0 + a/[1 + \exp(-(T - T_M)/b)]$, where $p(T)$ was the measured fluorescence value at a given temperature (T) and p_0, a, b, and T_M were constants.

Kinetics of ApoA-I/DMPC MLV Microsolubilization. The microsolubilization of MLV of DMPC containing various concentrations of cholesterol and oxysterols by apoA-I was measured as the decrease of vesicle turbidity followed by right-angle light scattering in a spectrofluorometer (*19*−*23*). Kinetic measurements were made by following the time-dependent reduction in right-angle light scattering (325 nm) due to the conversion of the large MLV (diameter ∼10000 Å) that scatter light to small rHDL (diameter ∼100 Å) that do not. The MLV were preincubated at the appropriate temperature and mixed with apoA-I to a final concentration of 0.5 mg of DMPC and 0.25 mg of apoA-I in a final volume of 3 mL. The samples were continuously stirred to prevent the settling of the vesicles. The data were analyzed to determine a kinetic half-time ($t_{1/2}$), which was the time required for a 50% decrease in the right-angle light scattering. Changes in right-angle light scattering do not directly correlate with the formation of rHDL because this measurement is predominately determined by the amount and size of the multilamellar vesicles present. Thus it is difficult to

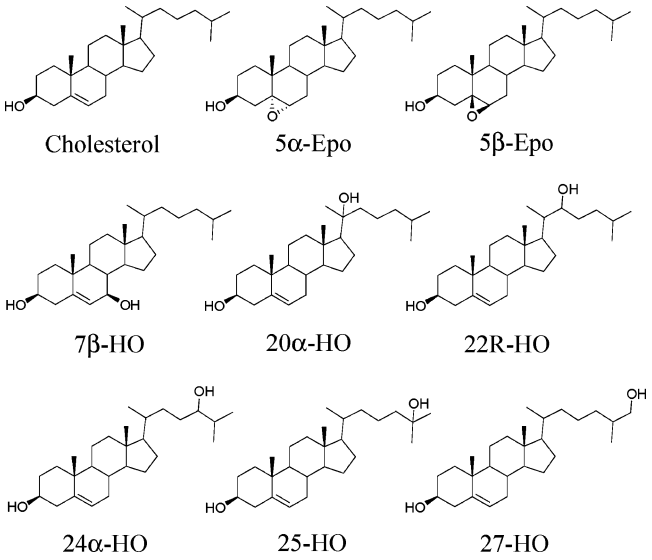

FIGURE 1: Structures of the sterols investigated: cholesterol, 5α,6α-epoxycholesterol (5α-Epo), 5*β*,6*β*-epoxycholesterol (5*β*-Epo), 7*β*-hydroxycholesterol (7*β*-HO), 20α-hydroxycholesterol (20α-HO), 22(*R*)-hydroxycholesterol (22R-HO), 24α-hydroxycholesterol (24α-HO), 25-hydroxycholesterol (25-HO), and 27-hydroxycholesterol (27-HO).

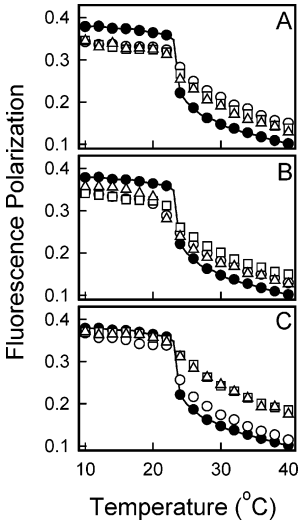

FIGURE 2: Effect of cholesterol and the oxysterols (10 mol %) on the DPH fluorescence polarization in DMPC MLV as a function of temperature: (A) cholesterol (○), 5α-Epo (□), and 5*β*-Epo (△); (B) 7*β*-HO (○), 20α-HO (□), and 22R-HO (△); (C) 24α-HO (○), 25-HO (□), and 27-HO (△); (A−C) no sterol (●). Every other temperature point is shown in the curves.

analyze the data as one type of process (i.e., single exponential) when the apparent rates vary so greatly. The reproducibility of the measured half-times for multiple samples of DMPC multilamellar vesicles have demonstrated that the values were within ±15% of each other. The apparent rate of microsolubilization of DMPC MLV was defined as rate = $1/t_{1/2}$. The rHDL reaction products were characterized by nondenaturing polyacrylamide gel electrophoresis on 4−15% gradient gels (Bio-Rad Laboratories, Hercules, CA). High molecular weight standards of known diameter were used to estimate the size of the rHDL. rHDL were also analyzed by gel filtration chromatography using two Superose HR6 columns in tandem on a AKTA FPLC (Amersham Biosciences).

RESULTS

Oxysterol Chemical Structure. Among the sterols chosen for our studies (Figure 1), oxygen groups occur on both the sterol nucleus and the isooctyl side chain. 7*β*-HO, 5α-Epo, and 5*β*-Epo, which have oxygen moieties on the sterol nucleus, are formed nonenzymatically and are oxysterols found in oxidized LDL and in human atherosclerotic lesions (*1*−*4*). 20α-HO, 22R-HO, 24α-HO, 25-HO, and 27-HO, which have oxygen moieties on the isooctyl side chain, are formed enzymatically. These sterols are involved in regulating cholesterol homeostasis, cholesterol catabolism, and reverse cholesterol transport; 27-HO is the major oxysterol in human atherosclerotic lesions. Natural variations in the location of the oxygen moiety allow a straightforward study of oxysterol structure/function relationships that should have physiological relevance.

Fluorescence Studies on Oxysterols in DMPC Bilayers. In DMPC MLV, the DPH fluorescence polarization decreases sharply at the temperature for the transition from the gel to L_d phase (T_M = 24 °C; Figure 2A). As revealed by the DPH fluorescence polarization, cholesterol, 5α-Epo, 5*β*-Epo, 7*β*-HO, and 20α-HO altered the order of DMPC MLV similarly; below and above T_M, respectively, acyl chain order was decreased and increased by the addition of these sterols (Figure 2A,B; Table 1). These five sterols also modulated the phase transition in a similar way; compared to that of DMPC, the transitions were not as sharp, and the changes in polarization with the thermal transition (Table 1) were smaller. Below T_M, the effects of 22R-HO, 24α-HO, 25-HO, and 27-HO on lipid order were smaller than for cholesterol (Figure 2B,C); above T_M, 22R-HO and 24α-HO induced a small increase in the fluorescence polarization, whereas 25-HO and 27-HO increased the polarization to a greater extent than did cholesterol. The different sterols modified the T_M (midpoint temperature for a 50% change in polarization) to different degrees where 22R-HO was the only sterol which clearly lowered the temperature of the gel to L_d phase transition (Table 1).

Table 1: DPH Fluorescence Polarization Measurements in DMPC/Sterol MLV[a]

steroid	T_M (°C)	*P* (15 °C)	*P* (35 °C)
none	24.3	0.37 ± 0.012	0.12 ± 0.003
cholesterol	26.8	0.33 ± 0.010	0.17 ± 0.006
5α-Epo	26.4	0.33 ± 0.011	0.16 ± 0.005
5*β*-Epo	25.8	0.33 ± 0.012	0.16 ± 0.005
7*β*-HO	24.9	0.33 ± 0.009	0.15 ± 0.005
20α-HO	25.9	0.33 ± 0.010	0.17 ± 0.006
22R-HO	24.1	0.35 ± 0.012	0.14 ± 0.005
24α-HO	25.4	0.35 ± 0.011	0.14 ± 0.005
25-HO	27.0	0.37± 0.013	0.21 ± 0.007
27-HO	27.1	0.37 ± 0.012	0.20 ± 0.006

[a] T_M is the temperature of the midpoint of the thermal transition, which corresponds to a 50% change in polarization. *P* is the DPH polarization at 15 and 35 °C. Values for *P* are the average values and standard deviation for triplicate samples.

Kinetics of Microsolubilization of DMPC MLV by ApoA-I. ApoA-I spontaneously associates with and solubilizes DMPC MLV forming rHDL with defined structures and stoichiometries. The rate of microsolubilization ($1/t_{1/2}$) is fastest at T_M where gel and L_d phases coexist and is enhanced by the addition of up to 10 mol % cholesterol (*19*−*21*). We

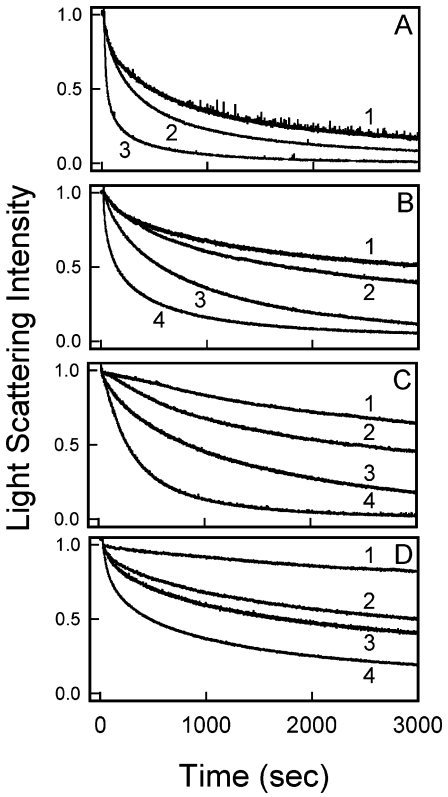

FIGURE 3: Kinetics of the apoA-I microsolubilization of DMPC MLV containing cholesterol and different oxysterols (5 mol %): (A, B) $T = T_M$ (24.0 °C); (C) $T < T_M$ (22.0 °C); (D) $T > T_M$ (26.0 °C) of DMPC; (A) 7β-HO (curve 1), no sterol (curve 2), and cholesterol (curve 3); (B) 22R-HO (curve 1), 27-HO (curve 2), 25-HO (curve 3), and 24α-HO (curve 4); (C) no sterol (curve 1), 27-HO (curve 2), 24α-HO (curve 3), and 20α-HO (curve 4); (D) no sterol (curve 2), 27-HO (curve 1), 20α-HO (curve 3), and cholesterol (curve 4). At 22.0 °C, the kinetic trace for cholesterol (data not shown) was essentially identical to that for 20α-HO.

Table 2: Half-Times ($t_{1/2}$) for Microsolubilization of DMPC/Sterol MLV by ApoA-I

sterol	$t_{1/2}$ (min), 5 mol %, $T = 24$ °C	$t_{1/2}$ (min), 10 mol %, $T = 24$ °C	$t_{1/2}$ (min), 5 mol %, $T = 22$ °C	$t_{1/2}$ (min), 5 mol %, $T = 26$ °C
none	5.0		93	70
cholesterol	0.85	0.56	4.3	7.4
5α-Epo	0.90	0.71	5.4	15
5β-Epo	1.1	1.1	4.1	26
7β-HO	7.7	10	3.7	35
20α-HO	4.0	6.6	4.2	28
22R-HO	51		4.9	300
24α-HO	1.5	1.0	14	18
25-HO	7.3	8.0	22	51
27-HO	31	100	39	250

compared the effects of cholesterol with those of various oxysterols on the kinetics of this process below (22.0 °C), at (24.0 °C), and above (26.0 °C) T_M. At T_M, the rate of microsolubilization was faster than those observed above and below T_M and was increased with the addition of 5 mol % cholesterol, 5α-Epo, 5β-Epo, 20α-HO, and 24α-HO but decreased with the addition of 5 mol % 7β-OH, 22R-HO, 25-HO, and 27-HO (Figure 3A,B; Table 2); the sterol-induced increases and decreases were dose dependent (Table 2). Below T_M, where DMPC is in the gel phase, the rates are slow but greatly enhanced by addition of 5 mol % oxysterol (Figure 3C), decreasing in the order cholesterol = 5α-Epo = 5β-Epo = 7β-HO = 20α-HO = 22R-HO > 24α-HO = 25-HO = 27-HO (Table 2). Above T_M, where DMPC is in a L_d phase, the rate of microsolubilization by apoA-I was slower than at T_M but increased with the addition of 5 mol % cholesterol, 5α-Epo, 5β-Epo, 7β-HO, 20α-HO, 24α-HO, and 25-HO (Figure 3D; Table 2). Interestingly, 5 mol % 22R-HO and 27-HO greatly reduced the rate of microsolubilization (Table 2).

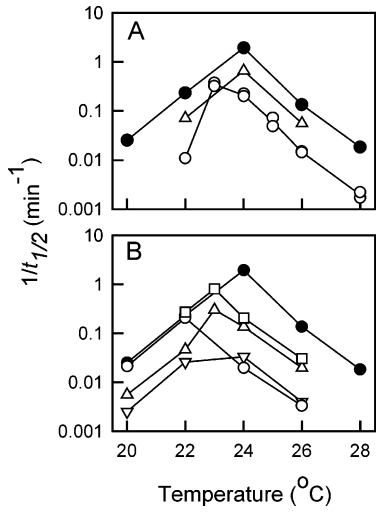

FIGURE 4: Rates of apoA-I microsolubilization of DMPC MLV containing different sterols (5 mol %) as a function of temperature. The apparent rate constants are expressed as $1/t_{1/2}$. Key: (A) no sterol (○), cholesterol (●), and 24α-HO (△); (B) cholesterol (●), 7β-HO (□), 25-HO (△), 22R-HO (○), and 27-HO (▽). Note that the $1/t_{1/2}$ values are on a logarithmic scale.

To correlate phase behavior of sterol/DMPC mixtures with lipid−apolipoprotein association, the temperature profiles for the rates of microsolubilization were determined for DMPC MLV containing various sterols. The maximum rate with respect to temperature for cholesterol and 24α-HO (and 5α-Epo and 5β-Epo; data not shown) was 24 °C, whereas the maximum rate for sterol-free MLV was ~23.5 °C (Figure 4A). For 7β-OH, 22R-OH, 25-HO, and 27-HO (and 20α-HO; data not shown) the maximum temperature was lower (Figure 4B). The combined effects of sterol structure and temperature on the rate of microsolubilization are profound, covering a range of nearly 3 orders of magnitude, with the fastest and slowest rates, respectively, observed at 5% cholesterol at T_M ($t_{1/2} = 51$ s) and 22R-HO above T_M ($t_{1/2} = 5$ h).

The membrane properties of DMPC MLV as assessed by DPH fluorescence polarization (Figure 2) were compared with the rates of apoA-I-mediated microsolubilization at 22 and 26 °C (Table 2). Below T_M, where the addition of sterol converts DMPC from gel to the less ordered L_o phase, the rate is constant at low polarization (i.e., more L_o phase lipids) but decreases at higher polarizations (i.e., less L_o phase lipids) (Figure 5A). Above T_M, where the addition of sterol can convert a L_d phase to a L_o phase, there was no correlation between bulk membrane properties and the rate of microsolubilization (Figure 5B). Addition of 5 mol % of the various sterols below and above T_M, respectively, was associated with rates that varied by factors of 20- and 40-fold.

Characterization of rHDL. Because sterol structure so dramatically affected the rate of rHDL formation, the reaction

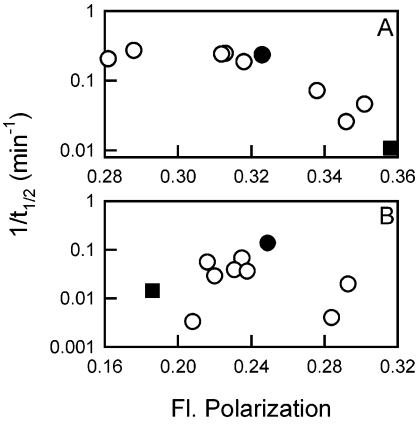

FIGURE 5: Comparison of the rates of apoA-I microsolubilization of DMPC MLV containing different sterols with membrane order as revealed by DPH fluorescence polarization. The rates ($1/t_{1/2}$) are from Table 2, and DPH polarization measurements are from Figure 2. Key: (A) 22 °C; (B) 26 °C; cholesterol (●), the oxysterols (○), and sterol-free MLV (■). Note that the $1/t_{1/2}$ values are on a logarithmic scale.

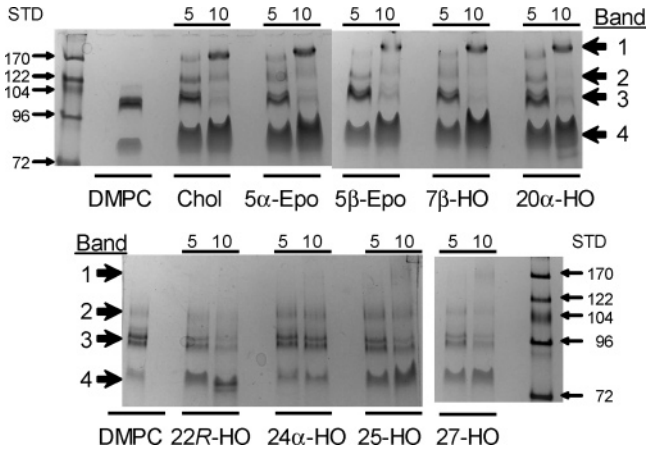

FIGURE 6: Nondenaturing PAGE (4−15% gradient) of rHDL formed from the microsolubilization of DMPC MLV by apoA-I. The apoA-I and DMPC (1/2 w/w) were mixed and incubated at 24 °C for 18 h. The lanes are labeled according to the sterol and its concentration. High molecular weight standards (STD) with diameters of 72, 96, 104, 122, and 170 Å were used to estimate the mean diameters of rHDL in each band. Band 1, which was found mainly containing 10 mol % sterol, had an apparent size of ∼180 Å. Band 2, which was a major component in mixtures containing 5 mol % sterol, had an apparent size of ∼120 Å. Band 3, the major component in sterol-free and 5 mol % sterol lipid mixtures, had a size range of ∼94−103 Å, depending on the initial lipid composition. The intensity of band 4, lipid-free apoA-I, increased with mole percent sterol.

products were analyzed to determine if the structures of rHDL were also affected. When analyzed by nondenaturing gradient gel electrophoresis, bands corresponding to distinct particle sizes were observed. Although there were no sterol-specific differences in the rHDL formed at both 5 and 10 mol % sterol (Figure 6), there were obvious differences in the effects of sterol concentration. Four protein staining bands were observed. Band 1, which was found mainly when the lipid mixtures contained 10 mol % sterol, had an apparent size of ∼180 Å. Band 2, which was a major product formed from lipid mixtures containing 5 mol % sterol, had an apparent size of ∼120 Å. Band 3, the major component in sterol-free and 5 mol % sterol lipid mixtures, corresponded to a size range of ∼94−103 Å, which depended on the initial

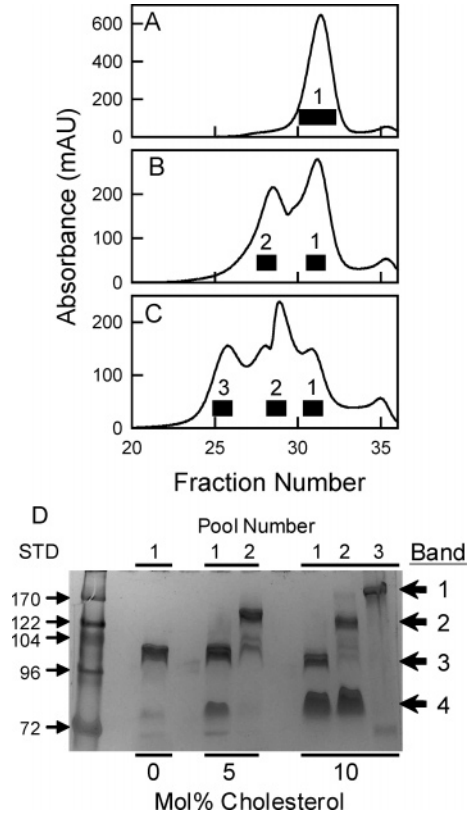

FIGURE 7: Effect of cholesterol content on the size of the rHDL formed by apoA-I microsolubilization of DMPC MLV. ApoA-I and DMPC MLV mixtures (1/2.5 w/w) containing (A) 0 mol %, (B) 5 mol %, and (C) 10 mol % cholesterol were incubated at 24 °C for 18 h and analyzed by Superose HR6 chromatography. Black bars represent the range of fractions that were pooled for analysis by nondenaturing PAGE. (D) Nondenaturing PAGE. By comparison with standards, the mean diameter of rHDL formed with no added cholesterol was 99 Å. rHDL formed from DMPC containing 5 mol % cholesterol had diameters of 99 Å (panel B, pool 1) and 135 Å (panel B, pool 2). rHDL formed from DMPC containing 10 mol % cholesterol had diameters of 96 Å (panel C, pool 1), 124 Å (panel C, pool 2), and 188 Å (panel C, pool 3). Increasing amounts of cholesterol increased the amounts of lipid-free apoA-I (band 4).

lipid composition; these could be separate but similarly sized particles. Band 4 was lipid- free apoA-I ,and the intensity of this band increased with the mole percent sterol in the starting mixture.

The effects of sterol concentration on the size and complexity of the rHDL particles were confirmed by Superose 6 HR size exclusion chromatography of the products formed from DMPC and various amounts of cholesterol. In the absence of added cholesterol, the rHDL was relatively homogeneous (Figure 7A). However, as the cholesterol content was increased, the elution profiles (Figure 7B,C) shifted to lower fraction numbers, which corresponded to larger particles. Specific column fractions were analyzed by nondenaturing PAGE (Figure 7D). In the absence of cholesterol, the rHDL had a mean diameter of 99 Å. rHDL formed from DMPC containing 5 mol % had mean diameters of 99 and 135 Å. At 10 mol %, the rHDL formed had mean diameters of 96, 124, and 188 Å. The amount of unassociated, i.e., lipid-free apoA-I, was also a function of the cholesterol concentration (band 4). The rHDL particles are similar to those prepared from apoA-I/cholesterol/DPPC reaction mixtures using a cholate removal method with

reported diameters of 97, 136, and 186 Å and two, three, and four molecules of apoA-I per particle (*37*).

DISCUSSION

Membrane surfaces can demonstrate considerable small-scale structural heterogeneity due to the formation of membrane domains of difference sizes and with different phase properties and domain boundary regions where there is a structural mismatch between the different lipid phases (*40*, *41*). Studies with artificial membranes have shown that membrane lattice defects that occur at domain boundaries are sites of high passive ion permeability (*42*−*46*), increased rates of phospholipid flip-flop (*47*) and protein insertion (*19*−*24*, *27*), and increased activities of surface-active enzymes such as phospholipases (*25*, *26*). The rate of microsolubilization of DMPC MLV by apoA-I is also highly dependent upon membrane surface properties and is fastest at the gel to L_d phase transition temperature, where molecules of apoA-I insert into defects in DMPC bilayers (*19*−*23*). The inverse correlation between apolipoprotein molecular weight and the insertion rate indicates that defect size is an important determinant of this process (*21*). According to this model, cholesterol increases the rate of association by forming a L_o phase, which in turn forms more phase boundaries and additional defects that are the sites of protein insertion (*20*). At a critical protein to lipid ratio at the bilayer surface, the bilayer is destabilized and portions "bud off", as rHDL (*24*). In this report, we investigate how the chemical structure of physiological oxysterols affects bilayer structure, the membrane association of apoA-I, and the formation of rHDL. One oxysterol, 7-ketocholesterol, inhibits apoA-I-mediated cholesterol efflux from macrophages, possibly by its effect on membrane properties; however, the precise mechanism is not known (*35*, *36*). Oxysterols also inhibit macrophage cholesterol efflux to HDL acceptors through a possible effect on the plasma membrane (*48*, *49*). Our studies in model membrane systems should have direct applicability to understanding the effect of plasma membrane domain structure on the pathways involving cellular cholesterol efflux.

Effect of Oxysterols on DMPC Phase Behavior. DPH fluorescence polarization identifies the well-known thermal transition from an ordered gel phase to a less ordered L_d phase (Figure 2). Like cholesterol, addition of 5α-Epo, 5*β*-Epo, 7*β*-HO, and 20α-HO to DMPC modulates this transition and reduces the order of the gel phase and increases the order of the L_d phase. 22R-HO and 24α-HO reduce and increase order below and above T_M, respectively, less than cholesterol. 25-HO and 27-HO have little effect on order below T_M but produce greater ordering than cholesterol above T_M (Figure 2; Table 1). The thermal transition identified by the midpoint of the change in DPH fluorescence polarization varied according to the identity of the sterol. Whereas the T_M for DMPC was 24.3 °C, the effects of added oxysterol varied from no change to an increase in T_M to ∼27 °C for 25-HO and 27-HO. More importantly, however, in the context of microsolubilization, the onset of melting did not follow the same pattern as the peak melting temperature. The onset of melting for DMPC bilayers containing no sterol, cholesterol, 5α-Epo, and 5*β*-Epo was similar (∼24 °C; Figure 2A), and the onset was slightly lower for 24α-HO, 25-HO, and 27-HO (∼23 °C; Figure 2C) and lowest for 7*β*-HO, 20α-HO, and 22R-HO (∼21 °C; Figure 2B).

In phospholipid bilayers, cholesterol is oriented quasi-perpendicular to the bilayer plane where the 3*β*-hydroxyl group is at the lipid−water interface and the isooctyl chain penetrates to the middle of the bilayer (*50*). The tight packing of cholesterol with phospholipids with saturated acyl chains is the basis for the formation of a L_o phase and the formation of membrane defects at the boundary that separates coexisting lipid phases (e.g., L_o and L_d phases). The effects of 5α-Epo, 5*β*-Epo, and 20α-HO on melting temperature and lipid order above and below T_M are similar to those of cholesterol, which suggest similar orientations in a bilayer. Although the addition of a second hydroxyl group does not introduce a large change in the shape of cholesterol, the potential for hydration by interfacial water could affect sterol orientation in the bilayer, thereby introducing a change in bilayer properties that is disproportionately large compared to the small change in covalent structure. Several physicochemical studies (*11*, *12*, *14*, *16*) indicate that 22R-HO, 25-HO, and 27-HO may have orientations within phospholipid bilayers which differ from cholesterol. In monolayer studies at low surface pressure, all three lie with their sterol nucleus parallel to the air−water interface so that both hydroxyl groups are hydrated. At higher surface pressures, 25-HO and 27-HO may assume an "inverse orientation" where the side chain hydroxyl group but not the 3*β*-hydroxyl group is at the air−water interface (*14*). Small-angle X-ray diffraction studies in oriented POPC bilayers indicated that 25-HO does not intercalate into the membrane hydrocarbon core and was primarily associated with the hydrated surface of the bilayer (*16*). Thus, the differential effects of oxysterols on membrane properties are expected to arise from how strongly the second oxygen moiety can be located at the lipid−water interface to orient the oxysterol in the bilayer to perturb DMPC packing.

Kinetics of DMPC Microsolubilization by ApoA-I Are Oxysterol Specific. The addition of oxysterols to DMPC MLV dramatically affected the rate of apoA-I-mediated microsolubilization. Under the experimental conditions of varying the temperature (between 20 and 28 °C) and with the addition of only 5 mol % sterol, the rates ($1/t_{1/2}$) varied over 3 orders of magnitude (Figure 4; Table 2). Cholesterol was the best sterol at enhancing the rate and, based on our proposed mechanism, formed a maximal number (and/or size) of membrane defects. Below T_M, the reaction of apoA-I with a gel phase DMPC matrix was very slow; however, it was dramatically increased upon the addition of sterol to form a coexisting L_o phase. All of the sterols enhanced the rate over sterol-free MLV, and 7*β*-OH, 20α-HO, 22R-HO, 25-HO, and 27-HO lowered the temperature at which the maximal rate occurred (Figure 4). These oxysterols also decreased the temperature for the onset of the thermal transition for DMPC. There was a trend that the rate is related to the amount of gel phase lipid converted to L_o phase lipid (Figure 5A). Above T_M, where the DMPC matrix was in the L_d phase, the reaction was again very slow. However, the addition of cholesterol to introduce a coexisting L_o phase increases the rate. 5α-Epo, 5*β*-Epo, 7*β*-HO, 20α-HO, 24α-HO, and 25-HO enhanced the rate over sterol-free MLV but were 2−6-fold slower than cholesterol. Surprisingly, the rates for 22R-HO and 27-HO were 3− 4-fold slower than for

sterol-free MLV. Additionally, there was no correlation of the rates with bulk membrane properties as measured by DPH polarization (Figure 5B). At T_M, where there is a mixture of gel and L_d phases, there was a dramatic increase in the rate for the pure DMPC matrix, and the rate was increased when cholesterol, 5α-Epo, 5β-HO, and 24α-HO were added to form a coexisting L_o phase. For these sterols the rate was also increased when the sterol concentration was increased to 10 mol % (Table 2). The other oxysterols were different in that they had both slower rates and the rates decreased even more when the sterol concentration was increased. In general, 5α-Epo, 5β-Epo, and 24α-HO demonstrated similar behavior to cholesterol. At all temperatures, the rates for 25-HO and 27-HO were dramatically lower than for cholesterol and for 22R-HO and 27-HO were slower than even sterol-free fluid MLV. The peculiar effects of these lipids may be a function of the membrane location of the hydroxyl groups, which if fully hydrated at the lipid−water interface would place them at the interfacial region of the bilayer where tight sterol/phospholipid packing, a requirement for domain formation, is minimized.

Sterol Concentration but Not Chemical Structure Determines rHDL Size. Although there were no sterol-specific effects on the size of rHDL, sterol concentration was a size determinant. rHDL with distinct diameters of 94−103, 120−135, and 180−188 Å were formed with the larger rHDL formed at higher sterol concentrations (Figures 6 and 7D). The sizes of these particles are remarkably similar to those formed in other systems. rHDL formed from mixtures of apoA-I/cholesterol/DPPC by the cholate dialysis removal method (*37*) have diameters of 97, 136, and 186 Å and two, three, and four molecules of apoA-I per particle, respectively; macrophage ABCA1-derived rHDL have diameters of ∼90, 120, and 150−160 Å (*33*); rHDL formed by stably transfected cells expressing ABCA1 have diameters of ∼120, 140, 170, and 190 Å (*38*). Our results demonstrate that sterol chemical structure determines the microstructure of the membrane surface which dramatically regulates the rate of rHDL formation, but sterol concentration determines the size of the particle formed. Thus, the formation of similar rHDL by spontaneous association of apoA-I with lipids (this study) and by the cholate removal method, which catalyzes this reaction, suggests that these rHDL as well as those derived from the ABCA1 pathway are thermodynamic products with compositions and dimensions that were determined solely by lipid composition.

Physiological Significance. An initial step in the formation of HDL is the lipidation of apoA-I by the ABCA1 lipid transporter (*28*−*31*). This process is not apoA-I specific since other apolipoproteins with amphipathic α-helices elicit similar effects (*51*, *52*). The mechanism for ABCA1-mediated lipidation of apoA-I is unknown; however, it probably involves both protein−protein interactions between apoA-I and ABCA1 and lipid−protein interactions between apoA-I and the membrane surface (*53*). One mechanism proposes a membrane microsolubilization step whereby apoA-I simultaneously removes phospholipid and cholesterol from lipid domains in whatever proportions they are present (*32*, *33*). Additionally, ABCA1 cycling between the plasma membrane and endosomal compartments is important for cholesterol efflux (*54*, *55*). Like other ABC transporters, ABCA1 is thought to pump phospholipids and possibly cholesterol from one leaflet of the membrane bilayer to the other in an energy-dependent way. This creates an imbalance in the phospholipid number between the two leaflets which would increase the lateral pressure and induce positive membrane curvature (membrane would bud out) in lipid domains adjacent to ABCA1 (*56*). Cells overexpressing ABCA1 have been demonstrated to have plasma membrane protrusions, the cells resembling echinocytes, which form when there are excess lipids in the outer membrane hemileaflet (*57*). ApoA-I and other apolipoproteins may bind to these perturbed membrane domains. Our studies suggest that ABCA1 could induce a membrane environment (e.g., domain formation) that overcomes the kinetic limitation of apoA-I−membrane association. In our model membrane system, there are dramatic sterol-specific effects on the rate of rHDL formation with some sterols being catalytic while others are inhibitory (Table 2). This is clearly important for DMPC bilayers above T_M, and possibly for the plasma membrane, where L_d and L_o domains coexist. The sterol composition and concentration of lipid domains created by ABCA1-mediated lipid transport could determine the membrane association of apoA-I as well as the size of the nascent HDL particle formed (*33*, *35*, *36*). Numerous structure/function studies have been used to separate out specific effects of cholesterol and other sterols in binding to protein regulatory or active sites (*58*, *59*) and supporting or inhibiting membrane raft formation (*5*−*9*, *60*). Similarly, we have developed a sterol structure/function relationship involving rHDL formation that can be used to systematically probe membrane structure to delineate the steps by which lipid-free apoA-I forms rHDL through the ABCA1 pathway.

In summary, these studies reveal, in part, the complexities of sterol−lipid interactions, even in the presence of presumably minor differences in structure. Our data, as well as data from other studies, show that sterols can promote or disrupt membrane domain formation; our studies further show that different lipid phases, which are sometimes a function of the structure of the phospholipid headgroup and acyl chain composition, dramatically alter sterol−phospholipid interactions. Finally, our studies demonstrate that the unique properties of the boundary region between coexisting membrane domains can dramatically regulate protein−membrane association.

REFERENCES

1. Bjorkhem, I., and Diczfalusy, U. (2002) Oxysterols: friends, foes, or just fellow passengers?, *Arterioscler. Thromb. Vasc. Biol. 22*, 734−742.
2. Olkkonen, V. M., and Lehto, M. (2004) Oxysterols and oxysterol binding proteins: role in lipid metabolism and atherosclerosis, *Ann. Med. 36*, 562−572.
3. Panini, S. R., and Sinensky, M. S. (2001) Mechanisms of oxysterol-induced apoptosis, *Curr. Opin. Lipidol. 12*, 529−533.
4. Leonarduzzi, G., Sottero, B., and Poli, G. (2002) Oxidized products of cholesterol: dietary and metabolic origin, and proatherosclerotic effects, *J. Nutr. Biochem. 13*, 700−710.
5. Xu, X., and London, E. (2000) The effect of sterol structure on membrane lipid domains reveals how cholesterol can induce lipid domain formation, *Biochemistry 39*, 843−849.
6. Xu, X., Bittman, R., Duportail, G., Heissler, D., Vilcheze, C., and London, E. (2001) Effect of the structure of natural sterols and sphingolipids on the formation of ordered sphingolipid/sterol domains (rafts). Comparison of cholesterol to plant, fungal, and disease-associated sterols and comparison of sphingomyelin, cerebrosides, and ceramide, *J. Biol. Chem. 276*, 33540−33546.

7. Wenz, J. J., and Barrantes, F. J. (2003) Steroid structural requirements for stabilizing or disrupting lipid domains, *Biochemistry 42*, 14267−14276.
8. Li, X. M., Momsen, M. M., Brockman, H. L., and Brown, R. E. (2003) Sterol structure and sphingomyelin acyl chain length modulate lateral packing elasticity and detergent solubility in model membranes, *Biophys. J. 85*, 3788−3801.
9. Wang, J., Megha, and London, E. (2004) Relationship between sterol/steroid structure and participation in ordered lipid domains (lipid rafts): implications for lipid raft structure and function, *Biochemistry 43*, 1010−1018.
10. Halling, K. K., and Slotte, J. P. (2004) Membrane properties of plant sterols in phospholipid bilayers as determined by differential scanning calorimetry, resonance energy transfer and detergent-induced solubilization, *Biochim. Biophys. Acta 1664*, 161−171.
11. Gallay, J., de Kruijff, B., and Demel, R. A. (1984) Sterol-phospholipid interactions in model membranes. Effect of polar group substitutions in the cholesterol side-chain at C20 and C22, *Biochim. Biophys. Acta 769*, 96−104.
12. Theunissen, J. J., Jackson, R. L., Kempen, H. J., and Demel, R. A. (1986) Membrane properties of oxysterols. Interfacial orientation, influence on membrane permeability and redistribution between membranes, *Biochim. Biophys. Acta 860*, 66−74.
13. Verhagen, J. C., ter Braake, P., Teunissen, J., van Ginkel, G., and Sevanian, A. (1996) Physical effects of biologically formed cholesterol oxidation products on lipid membranes investigated with fluorescence depolarization spectroscopy and electron spin resonance, *J. Lipid Res. 37*, 1488−1502.
14. Kauffman, J. M., Westerman, P. W., and Carey, M. C. (2000) Fluorocholesterols, in contrast to hydroxycholesterols, exhibit interfacial properties similar to cholesterol, *J. Lipid Res. 41*, 991−1003.
15. Smondyrev, A. M., and Berkowitz, M. L. (2001) Effects of oxygenated sterol on phospholipid bilayer properties: a molecular dynamics simulation, *Chem. Phys. Lipids 112*, 31−39.
16. Phillips, J. E., Geng, Y. J., and Mason, R. P. (2001) 7-Ketocholesterol forms crystalline domains in model membranes and murine aortic smooth muscle cells, *Atherosclerosis 159*, 125−135.
17. de Almeida, R. F., Loura, L. M., Fedorov, A., and Prieto, M. (2005) Lipid rafts have different sizes depending on membrane composition: a time-resolved fluorescence resonance energy transfer study, *J. Mol. Biol. 346*, 1109−1120.
18. Bacia, K., Schwille, P., and Kurzchalia, T. (2005) Sterol structure determines the separation of phases and the curvature of the liquid-ordered phase in model membranes, *Proc. Natl. Acad. Sci. U.S.A. 102*, 3272−3277.
19. Pownall, H. J., Massey, J. B., Kusserow, S. K., and Gotto, A. M., Jr. (1979) Kinetics of lipid−protein interactions: effect of cholesterol on the association of human plasma high-density apolipoprotein A-I with L-α-dimyristoylphosphatidylcholine, *Biochemistry 18*, 574−579.
20. Pownall, H. J., Massey, J. B., Kusserow, S. K., and Gotto, A. M., Jr. (1978) Kinetics of lipid−protein interactions: interaction of apolipoprotein A-I from human plasma high-density lipoproteins with phosphatidylcholines, *Biochemistry 17*, 1183−1188.
21. Pownall, H., Pao, Q., Hickson, D., Sparrow, J. T., Kusserow, S. K., and Massey, J. B. (1981) Kinetics and mechanism of association of human plasma apolipoproteins with dimyristoylphosphatidylcholine: effect of protein structure and lipid clusters on reaction rates, *Biochemistry 20*, 6630−6635.
22. McKeone, B. J., Pownall, H. J., and Massey, J. B. (1986) Ether phosphatidylcholines: comparison of miscibility with ester phosphatidylcholines and sphingomyelin, vesicle fusion, and association with apolipoprotein A-I, *Biochemistry 25*, 7711−7716.
23. Massey, J. B., and Pownall, H. J. (1998) Interaction of alpha-tocopherol with model human high-density lipoproteins, *Biophys. J. 75*, 2923−2931.
24. Segall, M. L., Dhanasekaran, P., Baldwin, F., Anantharamaiah, G. M., Weisgraber, K. H., Phillips, M. C., and Lund-Katz, S. (2002) Influence of apoE domain structure and polymorphism on the kinetics of phospholipid vesicle solubilization, *J. Lipid Res. 43*, 1688−1700.
25. Honger, T., Jorgensen, K., Biltonen, R. L., and Mouritsen, O. G. (1996) Systematic relationship between phospholipase A_2 activity and dynamic lipid bilayer microheterogeneity, *Biochemistry 35*, 9003−9006.
26. Jorgensen, K., Davidsen, J., and Mouritsen, O. G. (2002) Biophysical mechanisms of phospholipase A_2 activation and their use in liposome-based drug delivery, *FEBS Lett. 531*, 23−27.
27. Barlic, A., Gutierrez-Aguirre, I., Caaveiro, J. M., Cruz, A., Ruiz-Arguello, M. B., Perez-Gil, J., and Gonzalez-Manas, J. M. (2004) Lipid phase coexistence favors membrane insertion of equinatoxin-II, a pore-forming toxin from Actinia equine, *J. Biol. Chem. 279*, 34209−34216.
28. Yancey, P. G., Bortnick, A. E., Kellner-Weibel, G., de la Llera-Moya, M., Phillips, M. C., and Rothblat, G. H. (2003) Importance of different pathways of cellular cholesterol efflux, *Arterioscler. Thromb. Vasc. Biol. 23*, 712−719.
29. Oram, J. F. (2003) HDL apolipoproteins and ABCA1: partners in the removal of excess cellular cholesterol, *Arterioscler. Thromb. Vasc. Biol. 23*, 720−727.
30. Brewer, H. B., Jr., Remaley, A. T., Neufeld, E. B., Basso, F., and Joyce, C. (2004) Regulation of plasma high-density lipoprotein levels by the ABCA1 transporter and the emerging role of high-density lipoprotein in the treatment of cardiovascular disease, *Arterioscler. Thromb. Vasc. Biol. 24*, 1755−1760.
31. Lee, J. Y., and Parks, J. S. (2005) ATP-binding cassette transporter AI and its role in HDL formation, *Curr. Opin. Lipidol. 16*, 19−25.
32. Gillotte, K. L., Zaiou, M., Lund-Katz, S., Anantharamaiah, G. M., Holvoet, P., Dhoest, A., Palgunachari, M. N., Segrest, J. P., Weisgraber, K. H., Rothblat, G. H., and Phillips, M. C. (1999) Apolipoprotein-mediated plasma membrane microsolubilization. Role of lipid affinity and membrane penetration in the efflux of cellular cholesterol and phospholipid, *J. Biol. Chem. 274*, 2021−2028.
33. Liu, L., Bortnick, A. E., Nickel, M., Dhanasekaran, P., Subbaiah, P. V., Lund-Katz, S., Rothblat, G. H., and Phillips, M. C. (2003) Effects of apolipoprotein A-I on ATP-binding cassette transporter A1-mediated efflux of macrophage phospholipid and cholesterol: formation of nascent high-density lipoprotein particles, *J. Biol. Chem. 278*, 42976−42984.
34. Vedhachalam, C., Liu, L., Nickel, M., Dhanasekaran, P., Anantharamaiah, G. M., Lund-Katz, S., Rothblat, G. H., and Phillips, M. C. (2004) Influence of ApoA-I structure on the ABCA1-mediated efflux of cellular lipids, *J. Biol. Chem. 279*, 49931−49939.
35. Gaus, K., Dean, R. T., Kritharides, L., and Jessup, W. (2001) Inhibition of cholesterol efflux by 7-ketocholesterol: comparison between cells, plasma membrane vesicles, and liposomes as cholesterol donors, *Biochemistry 40*, 13002−13014.
36. Gaus, K., Kritharides, L., Schmitz, G., Boettcher, A., Drobnik, W., Langmann, T., Quinn, C. M., Death, A., Dean, R. T., and Jessup, W. (2004) Apolipoprotein A-1 interaction with plasma membrane lipid rafts controls cholesterol export from macrophages, *FASEB J. 18*, 574−576.
37. Wald, J. H., Krul, E. S., and Jonas, A. (1990) Structure of apolipoprotein A-I in three homogeneous, reconstituted high-density lipoprotein particles, *J. Biol. Chem. 265*, 20037−20043.
38. Denis, M., Haidar, B., Marcil, M., Bouvier, M., Krimbou, L., and Genest, J. (2004) Characterization of oligomeric human ATP binding cassette transporter A1. Potential implications for determining the structure of nascent high-density lipoprotein particles, *J. Biol. Chem. 279*, 41529−41536.
39. Massey, J. B. (2001) Interaction of ceramides with phosphatidylcholine, sphingomyelin and sphingomyelin/cholesterol bilayers, *Biochim. Biophys. Acta 1510*, 167−184.
40. Simons, K., and Vaz, W. L. (2004) Model systems, lipid rafts, and cell membranes, *Annu. Rev. Biophys. Biomol. Struct. 33*, 269−295.
41. Mukherjee, S., and Maxfield, F. R. (2004) Membrane domains, *Annu. Rev. Cell Dev. Biol. 20*, 839−866.
42. Cruzeiro-Hansson, L., and Mouritsen, O. G. (1988) Passive ion permeability of lipid membranes modeled via lipid-domain interfacial area, *Biochim. Biophys. Acta 944*, 63−72.
43. Cruzeiro-Hansson, L., Ipsen, J. H., and Mouritsen, O. G. (1989) Intrinsic molecules in lipid membranes change the lipid-domain interfacial area: cholesterol at domain interfaces, *Biochim. Biophys. Acta 979*, 166−176.
44. Corvera, E., Mouritsen, O. G., Singer, M. A., and Zuckermann, M. J. (1992) The permeability and the effect of acyl-chain length for phospholipid bilayers containing cholesterol: theory and experiment, *Biochim. Biophys. Acta 1107*, 261−270.
45. Clerc, S. G., and Thompson, T. E. (1995) Permeability of dimyristoyl phosphatidylcholine/dipalmitoyl phosphatidylcholine bilayer membranes with coexisting gel and liquid-crystalline phases, *Biophys. J. 68*, 2333−2341.

46. Xiang, T. X., and Anderson, B. D. (1998) Phase structures of binary lipid bilayers as revealed by permeability of small molecules, *Biochim. Biophys. Acta 1370*, 64−76.
47. John, K., Schreiber, S., Kubelt, J., Herrmann, A., and Muller, P. (2002) Transbilayer movement of phospholipids at the main phase transition of lipid membranes: implications for rapid flip-flop in biological membranes, *Biophys J. 83*, 3315−3323.
48. Kilsdonk, E. P., Morel, D. W., Johnson, W. J., and Rothblat, G. H. (1995) Inhibition of cellular cholesterol efflux by 25-hydroxycholesterol, *J. Lipid Res. 36*, 505−516.
49. Gesquiere, L., Loreau, N., and Blache, D. (1997) Impaired cellular cholesterol efflux by oxysterol-enriched high-density lipoproteins, *Free Radical Biol. Med. 23*, 541−547.
50. Aussenac, F., Tavares, M., and Dufourc, E. J. (2003) Cholesterol dynamics in membranes of raft composition: a molecular point of view from ^{2}H and ^{31}P solid-state NMR, *Biochemistry 42*, 1383−1390.
51. Fitzgerald, M. L., Morris, A. L., Chroni, A., Mendez, A. J., Zannis, V. I., and Freeman, M. W. (2004) ABCA1 and amphipathic apolipoproteins form high-affinity molecular complexes required for cholesterol efflux, *J. Lipid Res. 45*, 287−294.
52. Yokoyama, S. (2005) Assembly of high-density lipoprotein by the ABCA1/apolipoprotein pathway, *Curr. Opin. Lipidol. 16*, 269−279.
53. Panagotopulos, S. E., Witting, S. R., Horace, E. M., Hui, D. Y., Maiorano, J. N., and Davidson, W. S. (2002) The role of apolipoprotein A-I helix 10 in apolipoprotein-mediated cholesterol efflux via the ATP-binding cassette transporter ABCA1, *J. Biol. Chem. 277*, 39477−39484.
54. Martinez, L. O., Agerholm-Larsen, B., Wang, N., Chen, W., and Tall, A. R. (2003) Phosphorylation of a pest sequence in ABCA1 promotes calpain degradation and is reversed by ApoA-I, *J. Biol. Chem. 278*, 37368−37374.
55. Neufeld, E. B., Stonik, J. A., Demosky, S. J., Jr., Knapper, C. L., Combs, C. A., Cooney, A., Comly, M., Dwyer, N., Blanchette-Mackie, J., Remaley, A. T., Santamarina-Fojo, S., and Brewer, H. B., Jr. (2004) The ABCA1 transporter modulates late endocytic trafficking: insights from the correction of the genetic defect in Tangier disease, *J. Biol. Chem. 279*, 15571−15578.
56. Graham, T. R. (2004) Flippases and vesicle-mediated protein transport, *Trends Cell Biol. 14*, 670−677.
57. Wang, N., Silver, D. L., Costet, P., and Tall, A. R. (2000) Specific binding of ApoA-I, enhanced cholesterol efflux, and altered plasma membrane morphology in cells expressing ABC1, *J. Biol. Chem. 275*, 33053−33058.
58. Zhang, Y., Yu, C., Liu, J., Spencer, T. A., Chang, C. C., and Chang, T. Y. (2003) Cholesterol is superior to 7-ketocholesterol or 7alpha-hydroxycholesterol as an allosteric activator for acyl-coenzyme A:cholesterol acyltransferase 1, *J. Biol. Chem. 278*, 11642−11647.
59. Radhakrishnan, A., Sun, L. P., Kwon, H. J., Brown, M. S., and Goldstein, J. L. (2004) Direct binding of cholesterol to the purified membrane region of SCAP: mechanism for a sterol-sensing domain, *Mol. Cell 15*, 259−268.
60. Westover, E. J., and Covey, D. F. (2004) The enantiomer of cholesterol, *J. Membr. Biol. 202*, 61−72.

BI051169Y